Optical total reflection and transmission with mode control in a dielectric subwavelength nanorod chain*

Li Hao(李 浩)[a)b)], Li Wei(李 伟)[a)†], Du Jun-Jie(杜俊杰)[a)], Wu Ai-Min(武爱民)[a)], Qiu Chao(仇 超)[a)b)], Sheng Zhen(盛 振)[a)], Wang Xi(王 曦)[a)], Zou Shi-Chang(邹世昌)[a)], and Gan Fu-Wan(甘甫烷)[a)‡]

[a)] *State Key Laboratory of Functional Materials for Informatics, Shanghai Institute of Microsystem and Information Technology, Chinese Academy of Sciences, Shanghai* 200050, *China*

[b)] *University of Chinese Academy of Sciences, Beijing* 100049, *China*

(Received 23 February 2013; revised manuscript received 23 April 2013)

We report a polarization dependent reflection phenomenon beyond the normal incidence with a subwavelength nanorod chain. Light waves of the transverse electric mode will be totally reflected while those of the transverse magnetic mode will transmit through. The total reflection or transmission phenomenon can be seen as a constructive or destructive interference of the incident field with the transverse mode field of the chain. With the low-loss feature and the ultra-compact characteristic, this structure may find applications in photonic circuits.

Keywords: nanorod, reflection

PACS: 78.67.Qa, 78.67.Pt, 61.46.Km **DOI:** 10.1088/1674-1056/22/11/117807

1. Introduction

Reflectors have drawn wide attention due to many applications in imaging, solar energy collection, laser cavities, etc. Metallic mirrors are used to reflect light over a broad range of frequencies. However, they suffer from high material absorption loss in both infrared and visible light regions, which may severely limit the performance of the reflector-based devices. To avoid the metallic loss, much effort has been devoted to the research of total or anomalous reflection based on all-dielectric structures, such as the conventional distributed Bragg reflectors (DBRs), bandgap-based photonic crystals,[1–5] and resonant gratings.[6] However, the scale issue (too large in size) due to the periodicity or the frequency issue (too narrow in frequency) due to the resonance effect is inevitable.

The developments in rod synthesis and the physical characterization of nanostructures have enabled the investigation of the optical properties of single nanoparticles and ordered arrays of closely spaced nanoparticles.[7–9] The properties of the structures have found many applications in physics and engineering, including light energy transfer,[10,11] light generation,[12,13] optical sensing and detection,[14] and nonlinear optics.[15,16] A large number of papers have reported the electromagnetic energy transport with the longitudinal mode which is parallel to the chain axis and the transverse mode which is perpendicular to the chain axis.[17–19] When illuminated in oblique incidence, the symmetric and antisymmetric mode balancing can induce a strong enhancement of the near-field intensity in nano antennas composed of nanorods.[20] Those works provide us a deep insight of the extraordinary properties of the nanorod chain.

Recently, we reported a negative transmission phenomenon with the controlled longitudinal (L) and transverse (T) modes.[21] With an elaborately designed structure, the two excited modes in the chain resulted in a finite vortex of energy flow in each rod, which finally left the 1st order transmission in the negative direction. The aim of this paper is to theoretically study the total reflection or transmission phenomenon where the L and T modes are sustained by an all-dielectric subwavelength-nanorod chain. When a plane wave strikes on the chain, both L and T modes are excited and exhibit different effects on the near-field and far-field intensities. The total reflection or transmission phenomenon in the far-field region can be seen as the destructive or constructive interference of the T mode field with the incident field. In addition, we will show that our reflector is ultra compact, broadband, and can totally reflect the polarized light beyond the normal incidence. The dependences of the behavior on the dielectric rod size, the interparticle spacing, and the incident angle of light will also be discussed.

*Project supported by the National Natural Science Foundation of China (Grant Nos. 61107031, 11104305, 11204340, and 61275112), the National High Technology Research and Development Program of China (Grant No. 2012AA012202), and the Science and Technology Commission of Shanghai Municipality, China (Grant Nos. 10DJ1400400, 11ZR1443700, and 11ZR1443800).

†Corresponding author. E-mail: waylee@mail.sim.ac.cn

‡Corresponding author. E-mail: fuwan@mail.sim.ac.cn

© 2013 Chinese Physical Society and IOP Publishing Ltd

2. Model and results

Let us start with the total reflection and transmission phenomenon. For simplicity, we consider the two-dimensional case with infinite height. An array of rods are arranged along the x direction, the separation between the adjacent particles is $a_0 = 445$ nm. The nanorods are made of GaN, whose real part of index (n_{GaN}) is about 2.5 in the blue light region, and the imaginary part is neglected. The surrounding medium is assumed to be air ($n_{\mathrm{air}} = 1$). The radius of the rod is $r = 125$ nm. Figure 1(a) shows the magnetic (H) field intensity pattern of the transverse electric (with the H field along the y direction) mode at wavelength $\lambda = 480$ nm, which is calculated by the multiple scattering theory.[22] The incident wave vector is marked by the white arrow. Notice that most of the light waves towards the z direction are reflected back by the layer of nanorods. In Fig. 1(b), we present the reflectivity of the transverse electric (TE) mode in the blue light region. For comparison, the reflectivity of a typical Ag film is also presented. In practical applications, GaN-based light emitting diodes (LEDs) are widely used, however the light extraction efficiency (LEE) is not sufficiently high because of the trapping of light inside the semiconductor.[23] One method to improve the LEE is depositing a silver film on the bottom of the LED. The reflection of the silver film results in more light being extracted from the top of the device. However, due to the metallic material absorption loss, the reflectivity of the typical Ag film is no more than 95%. With the rod array we can obtain an obviously higher reflectivity with the same semiconductor material. On the contrary, we obtain an almost opposite reflection effect for the other polarized wave, as shown in the bottom panel of Fig. 1(b). The transverse magnetic (TM) mode waves are completely separated with the TE mode waves, and the reflectivity is less than 5% from 450 nm to 500 nm. The different reflectivities for different polarized waves indicate the potential application for polarization suppression in light sources.

For studying the underlying physics of the total reflection or transmission phenomenon, the scattered fields of the L and T modes are presented in Fig. 2 when the chain is excited with a plane wave. The array made up of the nanorods supports two different modes: the transverse mode with the dipole moments oriented perpendicular to the chain axis, and the longitudinal mode with the dipole moments aligned with the chain axis.[17–19] Figure 2(b) shows that the scattered field of the L mode is an evanescent mode and decays along the z direction, which affects the near-field distribution most, while the T mode is a propagating mode which affects the far-field distribution most, as shown in Fig. 2(c). In Fig. 2(i), the field distribution in the far-field region along $x = 0$ is plotted for the incident field, scattered fields of L and T modes, and the total field (composed of the scattered fields of L and T modes and the incident field). Notice that the scattered field of the L mode is almost 0 in the far-field region and the total field mainly depends on the incident field and the scattered field of the T mode. In other words, the superposition of the incident field and the scattered field of the T mode forms the total reflection phenomenon as shown in Fig. 2(d). Similarly, for another polarization, one can notice from Fig. 2(j) that the scattered field of the L mode is almost 0 in the far-field transmission region, while the field of the T mode mostly concentrates on the transmission region. A total transmission phenomenon as shown in Fig. 2(h) can be obtained as a superposition of the incident field and the scattered field of the T mode. Thus we can conclude that the total reflection or transmission phenomenon originates from the constructive or destructive interference of the T mode field with the incident wave.

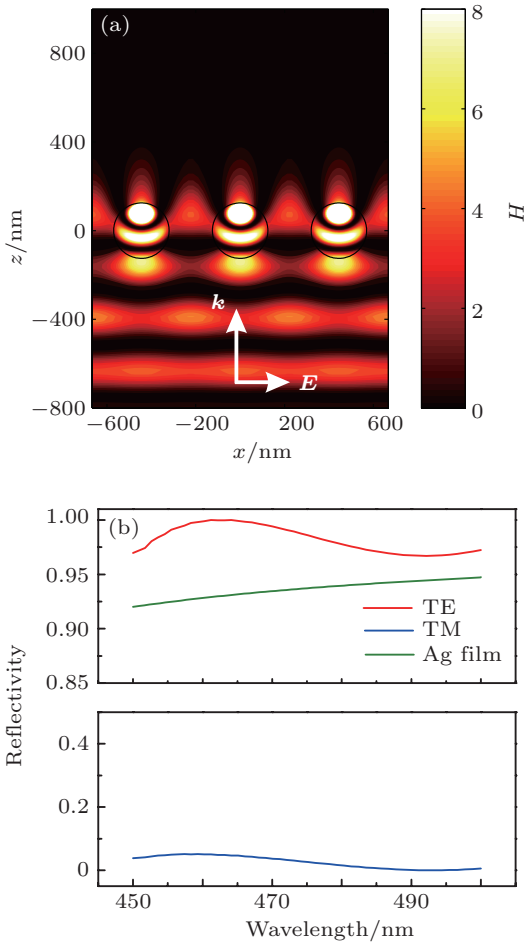


Fig. 1. (color online) (a) Distribution of H field intensity when a TE mode plane wave strikes on an array of nanorods in the x direction with radius $r = 125$ nm. (b)Reflectivity in the blue light region.

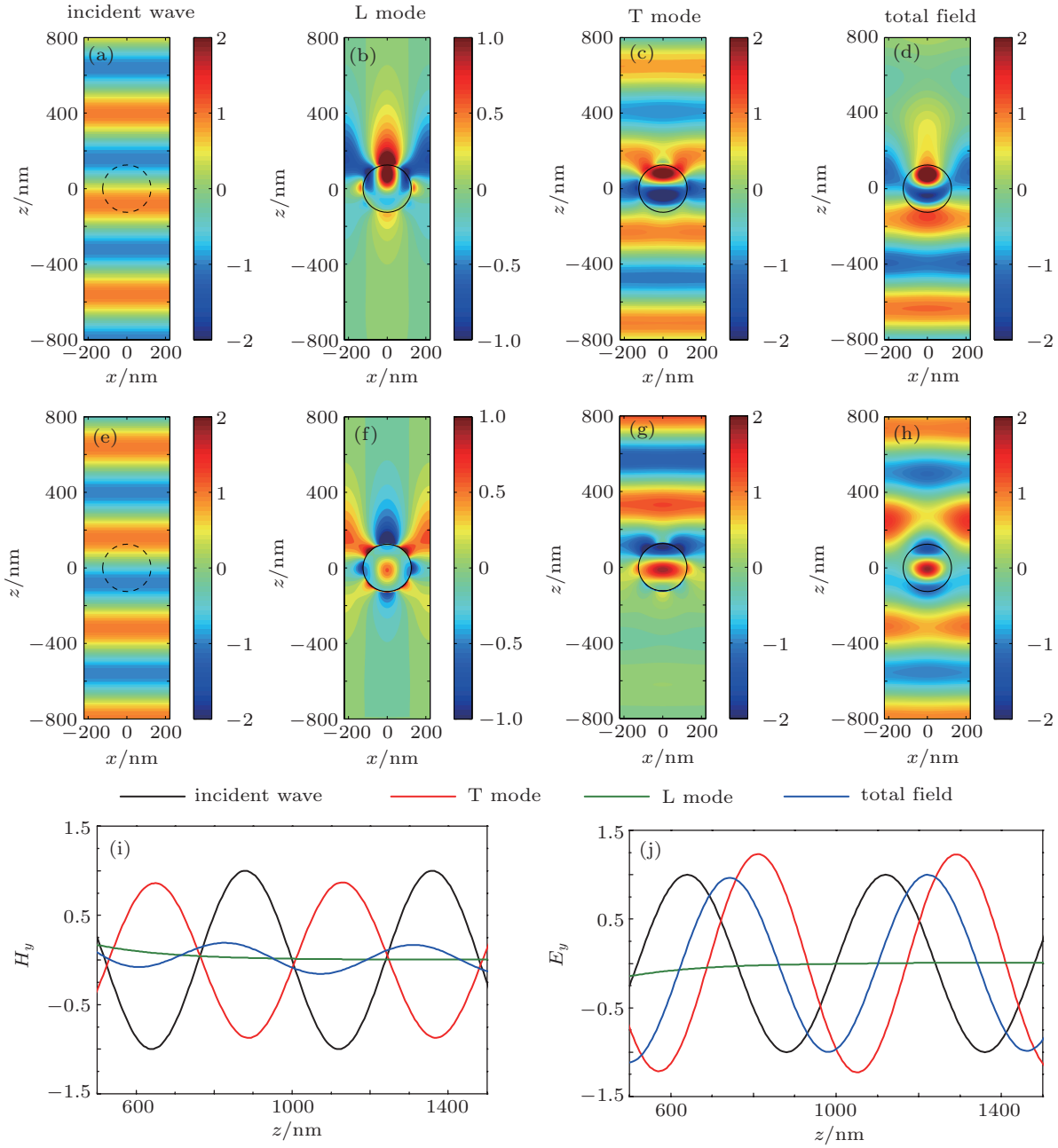


Fig. 2. (color online) TE waves: (a) the contour of H_y field distribution of the incident plane wave, the scattered fields of (b) L mode and (c) T mode, (d) the total field distribution. TM waves: (e) the contour of E_y field distribution of the incident plane wave, the scattered fields of (f) L mode and (g) T mode, (h) the total field distribution. The incident field, scattered fields of T and L modes, and total field distribution along $x = 0$ for (i) TE wave and (j) TM wave.

3. Analysis and discussion

Now we proceed to a rigorous calculation of the transmissivity and reflectivity by using the multiple scattering theory.[22] For simplicity, we consider a two-dimensional case with an array of nanorods. The nanorods are arrayed in the x direction with the l-th rod located at $R_l = la_0\boldsymbol{e}_x$. For transverse electric waves, with the magnetic (H) field polarized along the axis of the rod, the incoming and scattered H fields of rod l are expanded as

$$H_{\mathrm{i}}^{l} = \sum_{n=-\infty}^{+\infty} \mathrm{i}^n p_n^{(l)} \mathrm{J}_n(k_{\mathrm{b}} r_l)\, \mathrm{e}^{\mathrm{i}n\phi_l}, \tag{1}$$

$$H_{\mathrm{s}}^{l} = \sum_{n=-\infty}^{+\infty} \mathrm{i}^n a_n^{(l)} \mathrm{H}_n^{(1)}(k_{\mathrm{b}} r_l)\, \mathrm{e}^{\mathrm{i}n\phi_l}, \tag{2}$$

where $r_l = r - R_l = r_l(\sin\phi_l \boldsymbol{e}_x + \cos\phi_l \boldsymbol{e}_y)$, $p_n^{(l)} = \mathrm{e}^{-\mathrm{i}n\theta_i}\mathrm{e}^{\mathrm{i}k_{\mathrm{b}}R_l}$, J_n and $\mathrm{H}_n^{(1)}$ are the n-th order Bessel function and the Hankel function of the first kind, respectively, and k_{b} is the wave vector of the incident plane wave. By Floquet's theorem, $a_n^{(l)} = a_n^{(0)}\mathrm{e}^{\mathrm{i}k_x l a_0}$ with $k_x = k_{\mathrm{b}}\sin\theta_i$. A linear set of equations

can be obtained and solved for $a_n^{(0)}$. The reflected field is then given in terms of diffracted waves of different orders υ

$$H_{\rm r}(r) = \sum_{\upsilon} r_\upsilon \, {\rm e}^{{\rm i}(k_\upsilon x - \beta_\upsilon y)}, \tag{3}$$

with

$$r_\upsilon = \frac{2}{a_0}\frac{1}{\beta_\upsilon}\sum_{n=-\infty}^{+\infty}\frac{{\rm i}^n a_n^{(0)}(k_\upsilon - {\rm i}\beta_\upsilon)^n}{k_{\rm b}^n}. \tag{4}$$

Here $\beta_\upsilon = \sqrt{k_{\rm b}^2 - k_\upsilon^2}$ for $k_{\rm b}^2 \geq k_\upsilon^2$ and $\beta_\upsilon = {\rm i}\sqrt{k_\upsilon^2 - k_{\rm b}^2}$ for $k_{\rm b}^2 < k_\upsilon^2$, with $k_\upsilon = k_x + g_\upsilon$ and $g_\upsilon = 2\upsilon\pi/a_0$. Similary, one has the transmitted field

$$H_{\rm t}(r) = \sum_{\upsilon} t_\upsilon \, {\rm e}^{{\rm i}(k_\upsilon x + \beta_\upsilon y)}, \tag{5}$$

with

$$\begin{aligned} t_\upsilon &= t'_\upsilon + \delta_{\upsilon 0}, \\ t'_\upsilon &= \frac{2}{a_0}\frac{1}{\beta_\upsilon}\sum_{n=-\infty}^{+\infty}\frac{{\rm i}^n a_n^{(0)}(k_\upsilon + {\rm i}\beta_\upsilon)^n}{k_{\rm b}^n}. \end{aligned} \tag{6}$$

From Eqs. (4) and (6), we can obtain the reflectivity $R_\upsilon = |r_\upsilon|^2$ and transmissivity $T_\upsilon = |t_\upsilon|^2$ of different order diffraction. Meanwhile, the direction of different order diffraction is still determined by the classical grating.

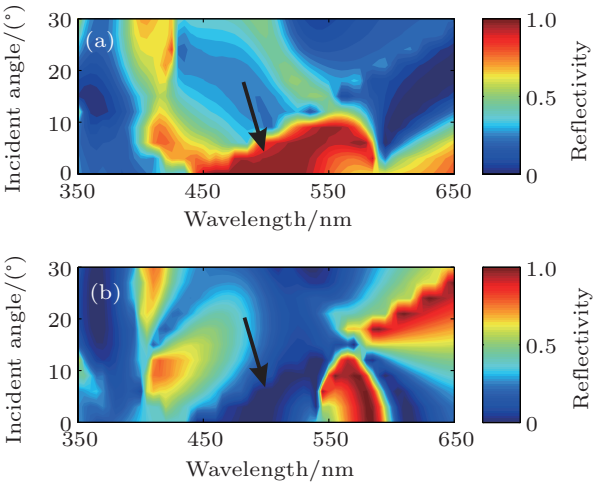


Fig. 3. (color online) The contours of reflectivity versus wavelength and incident angle for (a) TE mode and (b) TM mode. The total reflection and transmission regions are marked with the black arrows.

In most practical cases, the total reflection for the normal incidence is not useful. For our structure, the polarization dependent reflection phenomenon is not limited to the normal incidence case. We now consider the oblique incidence case with a small incident angle. The contours of reflectivity versus wavelength and incident angle for the TE and TM modes are presented in Figs. 3(a) and 3(b), respectively. The working regions of our structure are marked with the black arrows, corresponding to the total reflection and total transmission, respectively. Notice that the anomalous reflection phenomenon is not limited to the normal incidence, but within a certain incident angle range. The results illustrate that even for the oblique incidence, the high reflectivity and good polarization control can be obtained, providing a certain degree of angular tolerance for the reflector.

To give a clear design principle, we consider the structure with period $T = 445$ nm. The contours of reflectivity versus the radius of the rod and the incident wavelength are presented in Fig. 4. We pay our attention to the total reflection or transmission region for both modes, and the overlap region will be valuable to achieve specific applications. In our case, we choose region A (marked with the white arrow) in Fig. 4(a) to achieve a broadband reflection, while a total transmission for the TM mode is shown in the corresponding region of Fig. 4(b). By using region B, the TE waves will pass through while the TM waves are reflected back. Similarly, we can achieve the total reflection or transmission for both modes by choosing the working region appropriately.

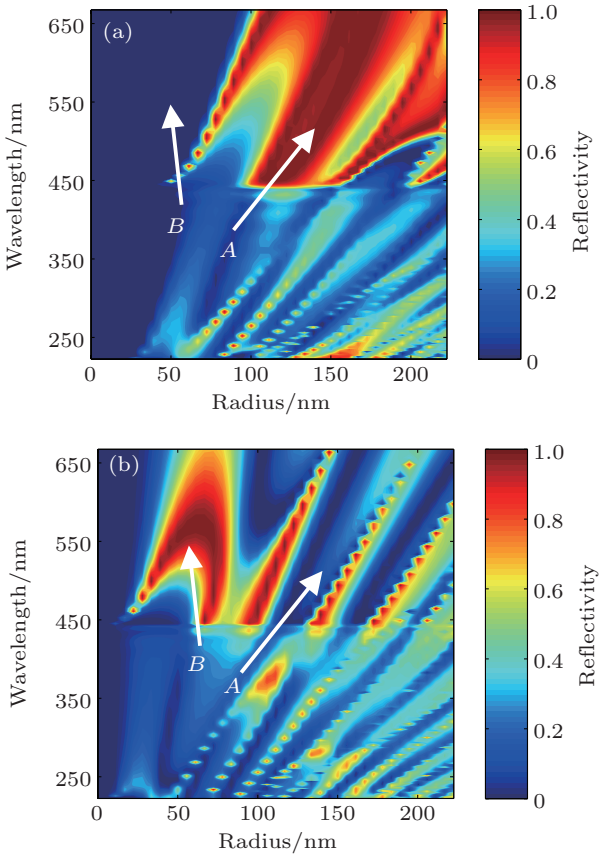


Fig. 4. (color online) The contours of reflectivity versus the radius of rod and the incident wavelength for (a) TE mode and (b) TM mode.

In addition, we can observe a clear boundary at wavelength $\lambda = 445$ nm. The broadband total reflection or transmission regions are mainly distributed above the boundary. The scattered fields of different diffraction orders are given by Eqs. (3) and (5). In this case (normal incidence: $\theta_{\rm i} = 0$), for the subwavelength structure ($\lambda > a_0$), only the 0-th order diffraction is propagating (β_0 is real), while the first, the

second, and the higher orders are all evanescent (β_0, β_1, etc are imaginary).[24] High reflectivity can be achieved in such a structure by merely suppressing the 0-th transmissive diffraction order (i.e., $t_0 = 0$). If there were more than one transmitted and reflected diffraction orders (i.e., when $\lambda < a_0$), obtaining high reflectivity ($|r_0|^2 \sim 1$) through the cancelation of multiple orders ($t_0 = 0$, $t_1 = 0$, $t_2 = 0$, etc) would be very difficult. Therefore, high reflectivity can be easily achieved because only the zeroth order diffraction needs to be suppressed for the subwavelength structure. The boundary in Fig. 4 at wavelength $\lambda = 445$ nm can be seen as the dividing line between the subwavelength structure and the ordinary structure.

In practical applications, a certain degree of size tolerance is necessary due to the imperfection of the fabrication technology or other factors. We turn our attention to the tolerance of the structure. Figures 4(a) and 4(b) also show the direct variation tendency of reflectivity with increasing radius. We notice that with increasing size of the nanorods, the working wavelength moves towards the long wavelength for both TE and TM modes. However, the broadband property makes this structure a certain degree of immunity to the wavelength moving. By assuming that the working wavelength is at $\lambda = 480$ nm, the fabrication tolerance of the diameter of the rod can be at least 10 nm.

4. Conclusion

To summarize, in this work, we present a wideband polarization dependent reflector with a subwavelength nanorod chain. Compared with the previous work, this structure offers an acceptable tolerance of incident angle and technical fabrication. With the compact characteristic and lossless material to operate in the optical frequency, it may provide us an alternative way to design the optical components in photonic circuits.

References

[1] Zhang Y J, Yang X Q, Han W and Xia Y J 2013 *Chin. Phys. B* **22** 090307
[2] Maystre D 2001 *Opt. Express* **8** 209
[3] Mocella V, Dardano P, Moretti L and Rendina I 2007 *Opt. Express* **15** 6605
[4] Lousse V, Suh W, Kilic O, Kim S, Solgaard O and Fan S 2004 *Opt. Express* **12** 1575
[5] Boutami S, Bakir B, Hattori H, Letartre X, Leclercq J L, Rojo-Romeo P, Garrigues M, Seassal C and Viktorovitch P 2006 *IEEE Photonics Technology Letters* **18** 835
[6] Peng S and Morris G M 1996 *Opt. Lett.* **21** 549
[7] Wang G T, Xue C S and Yang Z Z 2008 *Chin. Phys. B* **17** 1326
[8] Sun L F, Chen C Y, Sun L F, Zheng K H, Liu Z, Liu J and Hu L J 2010 *Chin. Phys. B* **19** 026101
[9] Shi S L, Liu Y G, Shi S L and Wang T H 2009 *Chin. Phys. B* **18** 4564
[10] Yariv A, Xu Y, Lee R K and Scherer A 1999 *Opt. Lett.* **24** 711
[11] Du J, Liu S, Lin Z, Zi J and Chui S T 2009 *Phys. Rev. A* **79** 051801
[12] Mazzitello K I, Mártin H O, Aldao C M and Roman H E 2004 *J. Phys. D: Appl. Phys.* **37** 668
[13] Laroche M, Albaladejo S, Carminati R and Sáenz J J 2007 *Opt. Lett.* **32** 2762
[14] Boriskina S V and Reinhard B M 2011 *Opt. Express* **19** 22305
[15] Marinica D C, Borisov A G and Shabanov S V 2007 *Phys. Rev. B* **76** 085311
[16] Xiao S, Su X R, Li C, Han Y B, Fang G J and Wang Q Q 2008 *Chin. Phys. B* **17** 1291
[17] Maier S A, Brongersma M L, Kik P G and Atwater H A 2002 *Phys. Rev. B* **65** 193408
[18] Maier S A, Kik P G and Atwater H A 2002 *Appl. Phys. Lett.* **81** 1714
[19] Crozier K B, Togan E, Simsek E and Yang T 2007 *Opt. Express* **15** 17482
[20] Devilez A, Stout B and Bonod N 2010 *Phys. Rev. B* **81** 245128
[21] Du J, Lin Z, Chui S T, Lu W, Li H, Wu A, Sheng Z, Zi J, Wang X, Zou S and Gan F 2011 *Phys. Rev. Lett.* **106** 203903
[22] Hulst H C 1981 *Light Scattering by Small Particles* (New York: Dover) pp. 297–232
[23] Wang P, Cao B, Gan Z and Liu S 2011 *J. Phys.: Conference Series* **276** 012083
[24] Li W, Chen J, Nouet G, Chen L and Jiang X 2011 *Appl. Phys. Lett.* **99** 051112